Bulk and interfacial superconductivity in lead and tin monochalcogenides: Majorana-like excitations in a ferromagnetic topological crystalline insulator

G.P.Mazur[1,2], K.Dybko[1], A.Szczerbakow[1], M.Zgirski[1], E.Lusakowska[1], S.Kret[1], J.Korczak[1], T.Story[1], M.Sawicki[1], and T.Dietl[2,1,3]

[1] *Institute of Physics, Polish Academy of Sciences, Warszawa, Poland*
[2] *International Research Centre MagTop, Warszawa, Poland*
[3] *WPI-Advanced Institute for Materials Research, Tohoku University, Sendai, Japan*

arXiv:1709:04000 gmazur@ifpan.edu.pl

As qubits resistant to local decoherence, Majorana bound states (MBSs) open prospects for fault-tolerant quantum computation. These zero-energy excitations are predicted to emerge at one-dimensional (1D) junctions of unconventional superconductors and topologically trivial systems, i.e., at the terminations of relevant 1D quantum wires or at boundaries, such as vortices, of 2D counterparts.Here we show, by using soft point-contact spectroscopy, that an electron-hole gap with a broad zero-bias conductance maximum develops at the topological surfaces of diamagnetic, paramagnetic, and ferromagnetic **$Pb_{1-y-x}Sn_yMn_xTe$**, where $y \gtrsim 0.67$ and $0 \leq x \leq 0.1$. The temperature dependence of the gap shows a critical behaviour with T_c up to 4.5 K, which however is not accompanied by a global superconductivity. We assign these findings to the presence of 1D topological states adjacent to surface atomic steps in topological crystalline insulators of IV-VI compounds[1]. Within this scenario, the interplay of carrier-carrier interactions, spin exchange with Mn ions, and pairing coupling within the flat 1D channels results in MBSs with lifted Kramers degeneracy, which are immune to the ferromagnetic ordering in the sample interior.

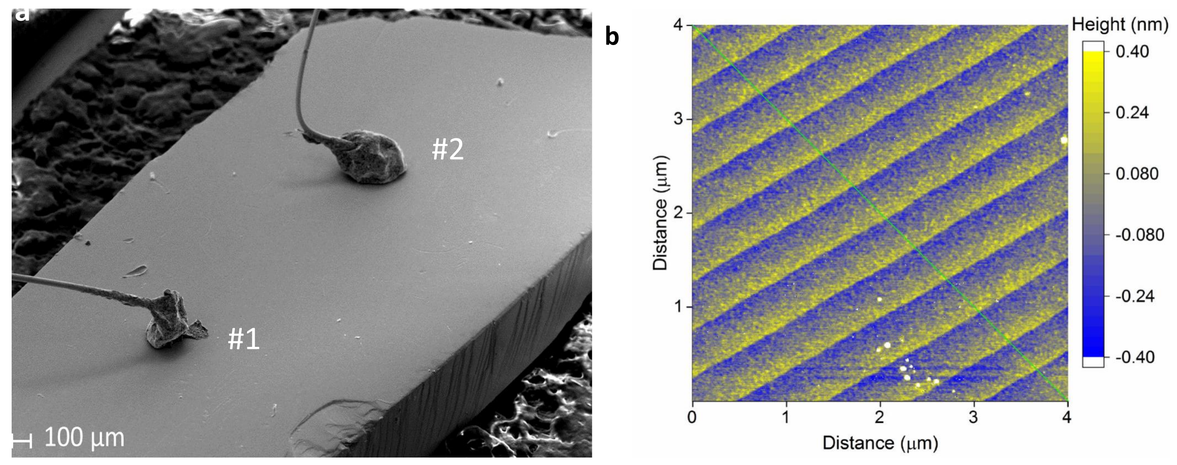

Fig. 3: (**a**) SEM image of the sample $Pb_{0.2}Sn_{0.8}Te$ with two soft point contact on the surface (An example of SPC measurements of topological superconductivity can be found in ref. 2). (**b**) AFM image of **atomic steps** (0.3 nm height) on as-grown $Pb_{0.2}Sn_{0.8}Te$ sample

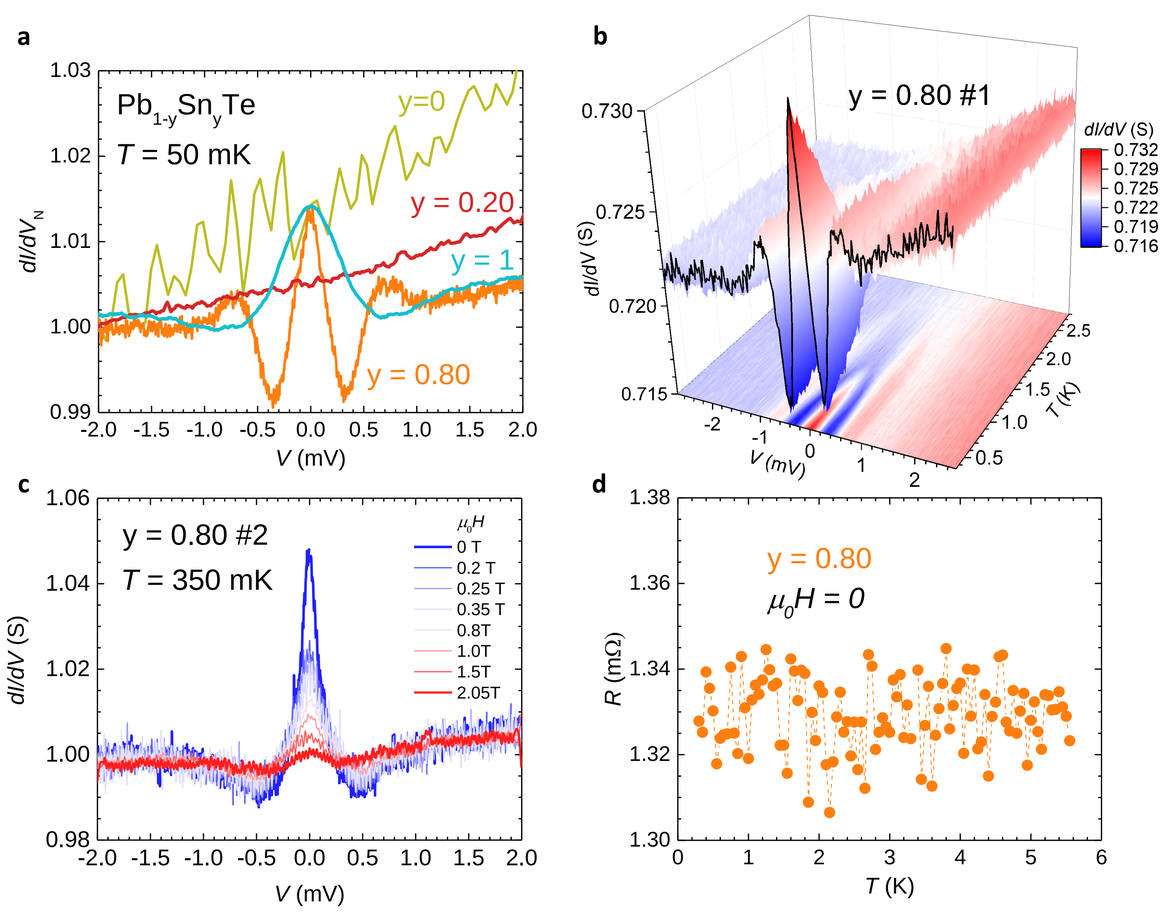

Fig. 1: Differential conductance spectra of soft point-contacts to diamagnetic samples. **a**, Differential conductance $\mathrm{d}I/\mathrm{d}V$ at 50 mK normalized to its value at the normal state for (001)$Pb_{1-y}Sn_yTe$ with $y = 0, 0.2, 0.8$, and 1. The spectrum is featureless for $y = 0$ (PbTe) and $y = 0.2$ but shows Majorana bound state-like characteristics for Sn content ($y = 0.8$ and 1, i.e., SnTe) corresponding to topological crystalline insulator phase. Evolution of the spectrum with temperature (**b**) and the magnetic field (**c**) for $y = 0.8$ and two locations of the point contact on the sample surface, respectively. Magnetic field is applied perpendicularly to the (001) plane. **d**, Resistance of this sample measured by a four contact method with current density as low as $2.5{\cdot}10^{-3}$ A/cm^2. No global superconductivity is detected.

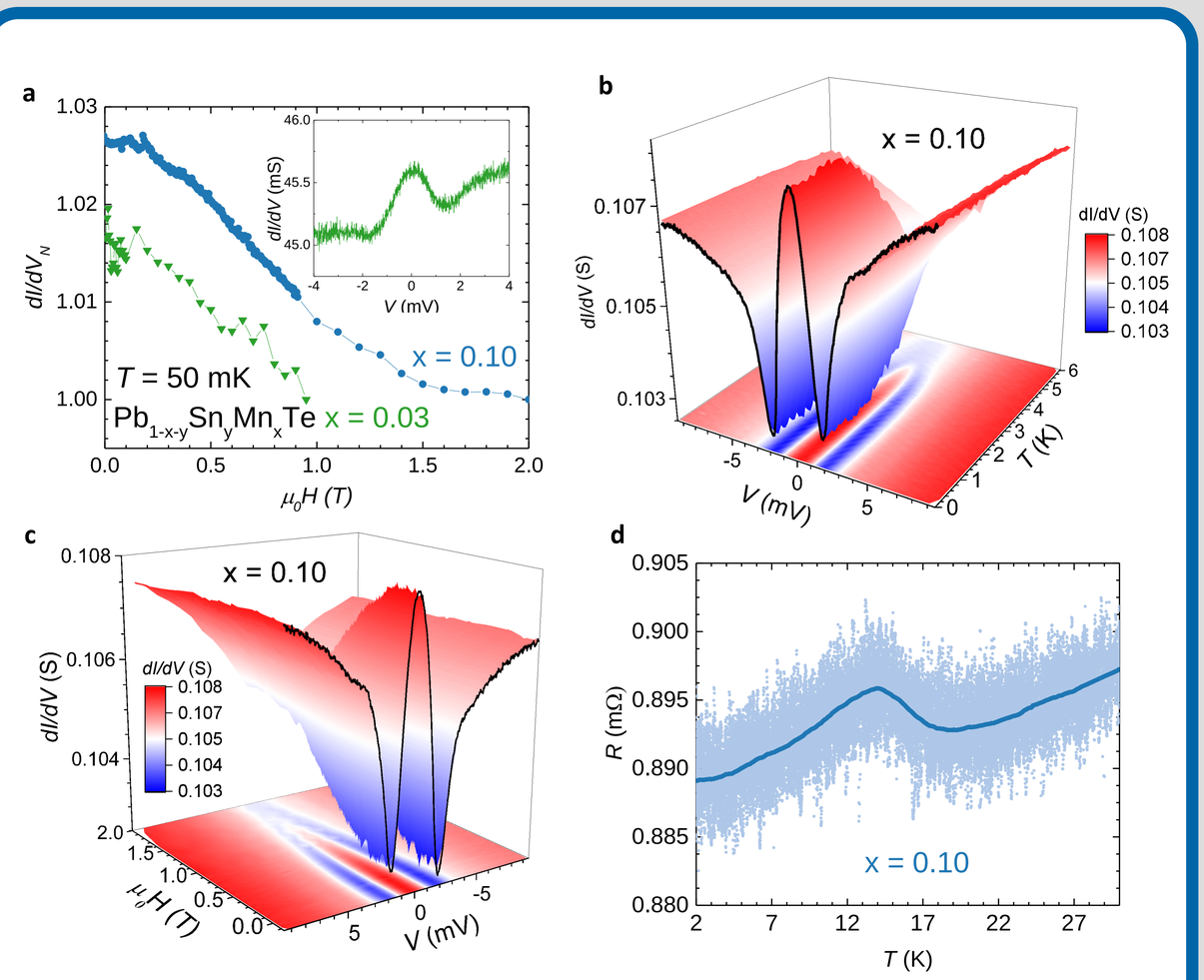

Fig. 4: Differential conductance spectra of soft point-contacts to paramagnetic and ferromagnetic samples showing Majorana-bound-state-type of behavior without global superconductivity. **a**, Normalized peak height field dependence for (011)$Pb_{0.30}Sn_{0.67}Mn_{0.03}Te$ and (011)$Pb_{0.16}Sn_{0.74}Mn_{0.10}Te$. Inset: conductance spectrum for (011)$Pb_{0.30}Sn_{0.67}Mn_{0.03}Te$ at 50 mK. Evolution of the spectrum with temperature (**b**) and the magnetic field (**c**) for (011)$Pb_{0.16}Sn_{0.74}Mn_{0.10}Te$. Magnetic field is applied perpendicularly to the (011) plane. **d**, Resistance of this sample was measured by a four contact method with current density $2.5 \cdot 10^{-5}$ A/cm^2 (noisy trace), solid line represents numerical average over 40 temperature scans. Critical scattering at the Curie temperature $T_{\mathrm{Curie}} = 14$ K is observed but no global superconductivity is detected.

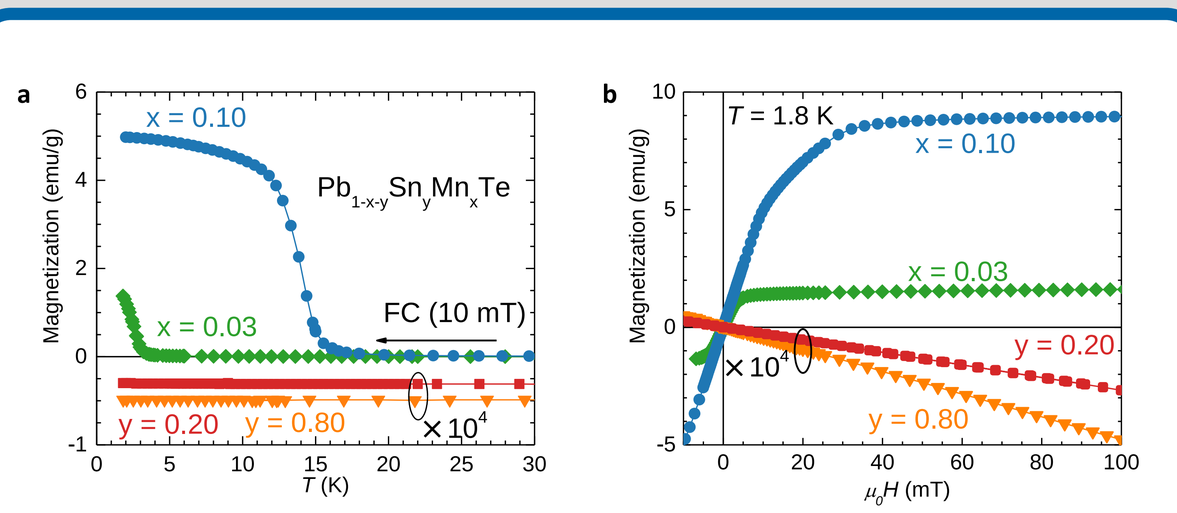

Fig. 2: Magnetization as a function of temperature (**a**) and the magnetic field (**b**) of $Pb_{1-y-x}Sn_yMn_xTe$ with various Mn concentrations x and the Sn content y. The data show the presence of ferromagnetism at low temperatures in Mn-doped samples with the Curie temperature increasing with x. Without Mn doping the samples are diamagnetic - in order to visualize the diamagnetism magnitude, the magnetization values are multiplied by a factor of 10^4.

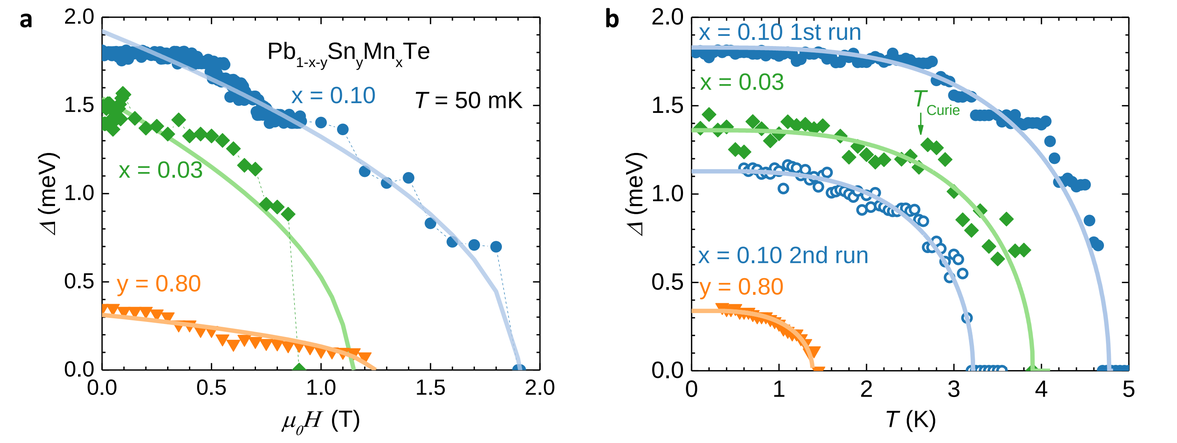

Fig. 5: Electron-hole gap Δ as a function of magnetic field (**a**) and temperature (**b**). Two sets of Δ values for $x = 0.10$ correspond to data taken in two series of measurements separated by heating of the sample to 10 K. Solid lines in (**a**) are fits of the formula $\Delta(T, H) = \Delta(T, H = 0)(1 - H/H_c)^{1/2}$. Magnetic field was applied perpendicular to the (011) plane for ferromagnetic samples and (001) for diamagnetic sample. Solid lines in (**b**) are fits of the BCS formula for $\Delta(T)$ to the experimental points treating T_c and C as adjustable parameters ($C = 4.38, 4.12, 4.44$, and 3.30 from top to bottom respectively; $C = 1.76$ in the BCS theory).

[1] Sessi, P. et al. Robust spin-polarized midgap states at step edges of topological crystalline insulators. *Science* **354**, 1269?-1273 (2016)

[2] Dziawa, P. et al. Topological crystalline insulator states in $Pb_{1-x}Sn_xSe$. *Nat. Mater.* **11**, 1023-1027 (2012)

[3] Sasaki, S. et al. Topological superconductivity in $Cu_xBi_2Se_3$. *Phys. Rev. Lett.* **107**, 217001 (2011)